17th World Conference on Earthquake Engineering, 17WCEE
Sendai, Japan - September 13th to 18th 2020

PARTIALLY REINFORCED MASONRY PIERS UNDER SEISMIC-TYPE LOADS. MEASUREMENTS AND NUMERICAL SIMULATIONS.

G.C. Manos [1], L. Melidis [2], K. Katakalos [3]

[1] *Emeritus Professor, Lab. Strength of Materials and Structures, Aristotle University, gcmanos@civil.auth.gr*
[2] *Postgraduate Student, Lab. Strength of Materials and Structures, Aristotle University, lazmelidis@gmail.com*
[1] *Assistant Professor, Lab. Strength of Materials and Structures, Aristotle University, kkatakal@civil.auth.gr*

Abstract

The main features of a study dealing with partially grouted reinforced clay brick masonry wall specimens are summarized here. Results from an experimental campaign studying the in-plane behavior of such partially grouted wall specimens, built using clay bricks with vertical holes manufactured by a local industry, are presented and discussed. All wall specimens were partially grouted at specific locations hosting vertical steel reinforcement. Horizontal (shear) steel reinforcement was also included at the mortar bed joints. These specimens were rigidly attached at a reaction frame and were subjected at their top to a constant vertical load together with a horizontal seismic-type cyclic load. The mechanical properties of all used materials were measured through laboratory tests. For the tested walls, with a height over length ratio equal to 1 and for horizontal reinforcing ratio values larger than 0.085%, the flexural response together with the rather ductile plastic rotation response at their bottom appeared to dominate the observed behavior when the maximum horizontal load was reached. A micro-modeling numerical simulation was per-formed with the bricks simulated by elastic plane finite elements separately from the mortar joints which were represented with non-linear links aimed to simulate the cut-off tensile capacity normal to the mortar joint -brick interface. The vertical reinforcement was simulated explicitly with non-linear links having mechanical properties based on the measured tensile characteristics of the actual reinforcement. The observed mainly flexural behavior was successfully reproduced by this micro-modeling numerical simulation featuring all the geometric and construction detailing together with the measured non-linear mechanical characteristics of the mortar joints and the vertical reinforcement of one tested specimen [1]. A key issue in the construction of these wall specimens is the masonry unit which is employed. Due to the thermal insulation requirements as well as the revisions in the provisions of the Euro-Code relevant to the seismic design and construction of unreinforced and reinforced masonry a novel masonry unit was designed and tested [2], [3], [4]. The design was based on preliminary material tests and a series of numerical simulations. The thermal insulation properties of this new unit were also taken into account in its design as well as the accommodation of the transverse horizontal joint reinforcement that was to be accommodated in a thin layer mortar joint. Summary results of all these aspects in the design and construction of this new masonry unit are present and discussed.

Keywords: Partially reinforced masonry, clay bricks, in-plane behavior, seismic-type loads, Tests-numerical response

Dedicated to the memory of the late Professor Hiroshi Akiyama of the University of Tokyo and the late Professor Heki Shibata of the Institute of Industrial Science, University of Tokyo.

1. Introduction

Extensive past research dealt with the performance of partially grouted reinforced masonry walls, when subjected to simulated seismic loads. Of particular interest is the in-plane seismic behavior. As was shown by Manos and co-workers (Manos 1983, Gulkan 1990) for low-rise well-built masonry structures, the in-plane behavior can be studied separately from the out-of-plane behavior. When subjecting such masonry walls simultaneously to combined in-plane horizontal and vertical loads (Hidalgo et al. 1978, Tomazevic et al. 1993), the most significant parameters that are usually examined are the type and strength of the mortar and masonry units, the geometry of the masonry walls and their reinforcing arrangement (in quantity and structural details), and the level of axial compression (Tasios 1987). Oan and Shrive (2009) examined the shear behavior of concrete masonry walls whereas Sandoval et al. (2018) investigated the in-plane cyclic response of partially grouted rein-forced clay brick masonry walls in a way similar to the one employed in the present work. A first objective of the present study is to validate the local mate-rials and construction practices towards building earthquake resistant low-rise partially grouted rein-forced clay brick masonry structures in areas of moderate seismicity of Greece (Manos 2000a, Manos 2000b). A second objective is to numerically simulate the observed behavior of such partially grouted reinforced masonry wall specimens. The following summarizes the main features of the experimental program with partially grouted reinforced clay brick masonry wall specimens (Manos 2000a).

2. Experimental program

This investigation examined the influence of the variation of the specimens' geometry, the mortar type, the horizontal and vertical reinforcement ratio values, the level of compressive axial load applied together with the horizontal force at the top of each specimen (pseudo-dynamic or dynamic in nature). This variation resulted in a considerable number of partially grouted reinforced masonry wall specimens. Almost all wall specimens were 154mm thick built with the clay brick unit shown in Figure 1. Specimen Wall-34N, which was 320mm thick, was also built with the same brick unit of Figure 1 (alternatively either two bricks or one brick forming the width of the wall). Most specimens were built with clay brick type C (see Figure 1). A small number of specimens were built with a slightly different clay brick (type D). The overall dimensions of both brick types were 154mm wide, 320mm long with a height of 155mm. According to Table 3.1. of Eurocode 6 (2005) both these clay bricks are classified as a group 2 masonry units. The measured values of the mechanical proper-ties of the all used materials are given in the next section.

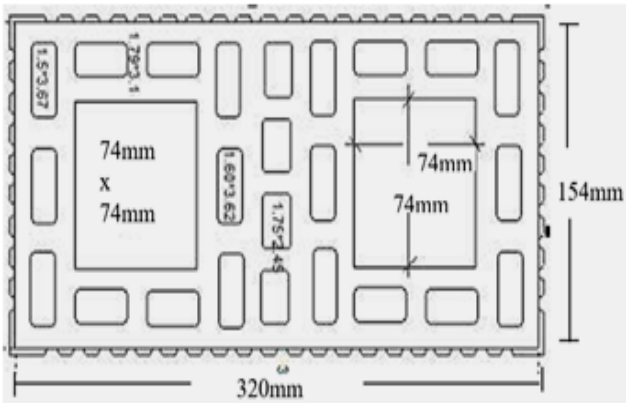

Figure 1: Type C clay brick

Gross area: 50560 mm2

Area of all holes: 48.6% of gross area.

Area of grip holes: 10.8% of gross area.

Area of each one of small holes: < 2% of gross area.

Thickness of internal web and external shell: 11mm > 8mm

. Minimum value of combined thickness webs and shells:

44mm > 16% of overall width

According to the provisions of Table 3.1. of Eurocode 6 this clay brick is classified as a group 2 masonry unit

The clay brick unit of Figure 1 was initially developed as a pilot masonry unit by the Filippou Structural Clay Products (Manos 2000a). Moreover, apart from the current study the potential of such a clay brick unit to be used for partially grouted reinforced masonry was also examined by Psylla et al., 1996.

a. Geometry: Most wall specimens (twenty-eight) were 1330mm long, 1330mm high and 154mm thick; these were relatively "wide" specimens with a height over length (h/l) ratio equal to 1. In addition, eight (8) specimens were 660mm long, 1330mm high and 154mm thick; these were relatively "slender" specimens with a height to length (h/l) ratio equal to 2. Apart from the above geometry, two specimens that were 2700mm long and 2475mm high were also tested. One of these specimens was 154mm thick (Wall-27N, Figure 4), representing a one-story high interior wall, whereas the second specimen with the same length and height was 320mm thick (Wall-34N), representing a one-story high exterior wall. Both these specimens had a height over length (h/l) ratio equal to 0.917. All tested wall specimens were constructed in running bond with bed joints and head joints approximately 10mm thick.

b. Mortar type. All wall specimens were selectively built with mortar types characterized by their compressive strength. A small number of specimens (six) used mortar with a target compressive strength

equal to 2.5MPa, representing a relatively weak mor-tar (marked with the letter O). Alternatively, mortar with a target compressive strength equal to 5.0MPa, representing a relatively strong mortar (marked with the letter N) was used for most specimens (thirty-two).

c. Variation of the longitudinal and / or transverse reinforcement. The amount of transverse (horizontal) reinforcement, in terms of ratio of the area of this reinforcement over the corresponding gross cross-sectional area, was varied from 0.05%, to 0.150%. For the largest specimens Wall-27N and Wall-34N the value of this ratio was equal to 0.102% and 0.097%, respectively. The amount of the longitudinal (vertical) reinforcement, in terms of ratio of the area of this reinforcement over the corresponding gross cross-sectional area of each wall specimen, was equal to 0.125% for most specimens. For Wall-27N and Wall-34N specimens the value of this ratio was equal to 0.086% and 0.082%, respectively

d. Variation of the vertical load imposed at the top of each specimen. Twenty-two specimens were subjected to 4% of the compressive strength of the brick masonry (fk) whereas eleven specimens were subjected to 8% of that strength. A limited number of specimens (three) were tested with no axial compression. The strength of each masonry type was found by testing masonry wallets constructed with the same clay brick unit using either weak (O) or relatively strong (N) mortar (see table 1 in the next section).

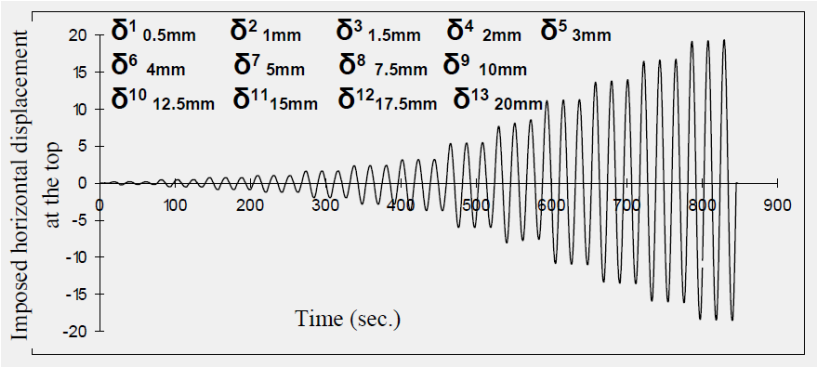

Figure 2: Imposed horizontal seismic-type loading sequence

e. Variation of the seismic-type load. The horizontal seismic-type load was imposed to each wall specimen together with the vertical compressive load. In all cases, this horizontal load was a series of three sinusoidal cycles of progressively increasing amplitude as depicted in Figure 2. In this figure the maximum amplitude at the end (13th step) of this horizontal sequence is 20mm and it is reached by thirteen (13) similar 3-cycle consecutive loading steps of continuously increasing amplitude. The amplitudes of each one of these thirteen 3-cycle loading steps are listed at the top of Figure 2. The frequency of each one of these cycles was kept constant. For thirty specimens, including large dimensions specimens Wall-27N and Wall-34N, the frequency of the horizontal loading cycles was equal to 0.048Hz, representing a pseudo-dynamic type of loading. For eight wall specimens the frequency of these loading cycles was much higher set equal to 1Hz thus representing a dynamic type of loading sequence.

3. Material characterization

The mechanical properties of the used clay brick units, mortar types O and N, horizontal and vertical reinforcing bars and grout were defined by laboratory testing of samples of the used materials taken during construction of the wall specimens described be-fore. Together with the construction of these wall specimens a number of wallets were also constructed using the same clay brick units and the same mortar types described before. These wallets, with dimensions listed in column (4) of table 1, were subjected to either axial or diagonal compression, as described in column (5) of the same table. Column 1 of this table lists the tested wallets, indicating with the letter N (strong mortar) or O (weak mortar) the used mor-tar type in their construction which was the same mortar used in the construction of the corresponding wall specimens described before. The corresponding measured mean compressive mortar strength value of these two mortar types is listed in column (2) of this table. The type of brick used for building these wallets is listed in column (3) of Table 1. At the bottom of this table the values of the normalized mean com-pressive strength of these clay brick units type C and D, as defined in Eurocode 6, is also listed. These values were found from compressive tests of these clay bricks in a direction normal to their cross-section (Figure 1) performed according to EN 772-1 (2011). The dimensions in millimeters of these wallets are listed in column 4, (height/length/thickness). From the maximum value of the axial or diagonal compressive load, measured during testing these wallets, the corresponding compressive strength (fk) and shear strength (fvk) values are derived and listed in column (6) of table 1. Column (7) of this table lists corresponding predicted values making use of the relevant provisions of Eurocode 6 (2005) together with the measured mortar compressive strength values (type N or O) and the measured clay brick unit (type C or D) compressive strength values. Listed is also the limit shear strength value for zero normal stress (fvko), for this type of mortar and clay brick units, according to table 3.4 of Eurocode 6. Use is made for predicting the compressive strength value fk of the following empirical formula (1) of Eurocode 6 (2005) as defined after the latest revision of this document, where fb is the normalized mean com-pressive strength of the brick unit in N/mm2 and fm is the compressive strength of the mortar, in N/mm2. The value of the constant K (K=0.45) is found ac-cording to table 3.3 of Eurocode 6 having previously ascertained that the clay brick unit belongs to group 2, according to table 3 of this document (see also Figure 1). Finally, the mean Young's modulus values found from the compressive tests of the wallets listed in table 1 are equal to 4000MPa for the wallets built with mortar type N and 3000MPa for those built with mortar type O.

$$f_k = K f_b^{0.7} f_m^{0.3} \qquad (1)$$

Deformable reinforcing bars with diameter either 8mm or 10mm were used as vertical reinforcement with measured mean yield stress 523MPa and 501MPa, respectively. The corresponding measured tensile strength values were 635MPa and 647MPa for these deformable reinforcing bars exhibiting a tensile strain of 11% at maximum load. Deformable reinforcing rods of 4mm diameter formed the horizontal reinforcement for most specimens with a measured yield stress and tensile strength equal to 590MPa and 757MPa, respectively. The mean measured grout compressive strength was equal to 9.35MPa and the mean measured bond strength was equal to 0.45MPa and 0.65MPa for the horizontal and vertical reinforcing bars, respectively.

4. Loading arrangement

Figure 3 depicts the testing layout whereby all wall specimens were placed, one at a time, within a steel reaction frame. The vertical load was kept almost constant at a predetermined level, whereas the horizontal displacement, applied at the top, was varied in a cyclic manner (Figure 2). When loaded, the specimen has its foundation anchored to the reaction frame. A reinforced concrete beam was built at the top fully connected to each specimen. The horizontal actuator was attached both to this concrete beam and to the reaction frame with a system of hinges in order to allow the in-plane top horizontal displacement and the in-plane rotation of the specimen during loading. The out-of-plane response of the specimen was prohibited with a system of roller-sliders.

Table 1: Compression and shear strengths derived from wallet tests

Specimen Name	Compr. Mortar Strength fm (MPa)	Brick Name	Dimensions of Pier (H/B) (mm)	Type of Test	Measured Strength (MPa)	Predicted Strength (MPa)
(1)	(2)	(3)	(4)	(5)	(6)	(7)
Wallet 2N	4.03	C	1300/663/155	Compression	4.56	3.385
Wallet 3N	4.03	C	1300/661/155	Compression	4.53	3.385
Wallet 5N	4.03	C	1295/655/155	Compression	5.10	3.385
Wallet 2O	2.09	C	1300/663/155	Compression	3.48	2.778
Wallet 3O	2.09	C	1295/663/155	Diagonal Tension	3.37	2.778
Wallet 2DO	2.09	D	660/660/155	Diagonal Tension	0.204	0.10
Wallet 2DN	4.03	D	975/1000/155	Diagonal Tension	0.24	0.15
Wallet 3DO	2.09	D	975/1000/155	Diagonal Tension	0.199	0.10
*fb = 9.82MPa For Brick C, fb = 7.85MPa For Brick D						

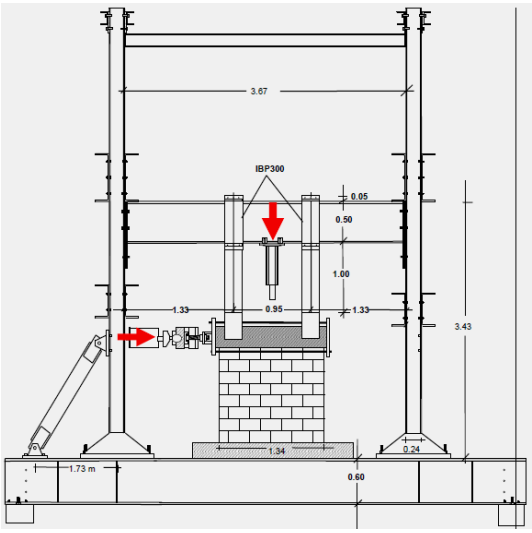

Figure 3: Masonry wall being subjected

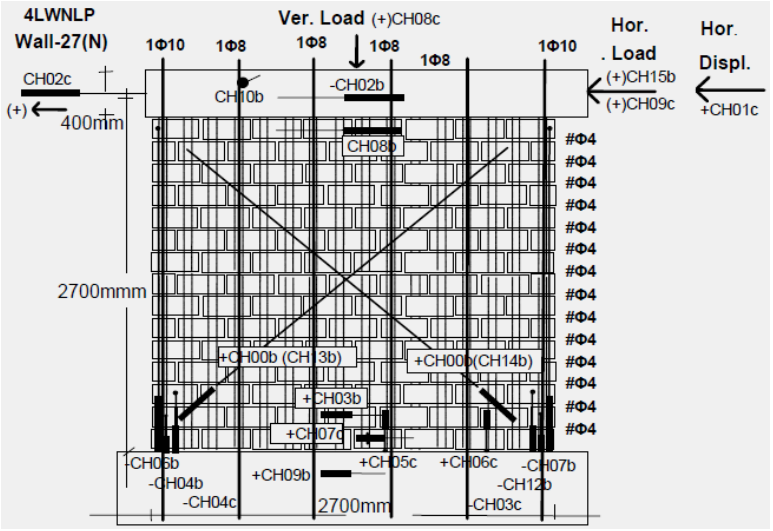

Figure 4: Typical reinforcing details of specimen Wall27N and instrumentation scheme

5. Construction details and instrumentation features

All specimens were constructed in accordance with standard practices of reinforced masonry construction regarding the laying of the bricks and mortar, the placement of the longitudinal (vertical) and bed-joint (horizontal) reinforcement and the pouring of the grout in the vertical cells. Figure 4 depicts the partial reinforcement of a typical wall-specimen. For all wall specimens with a height 1330mm the vertical reinforcement was anchored directly to the R/C foundation block, which was already cast before building the masonry. For walls specimens with a height 2700mm (Wall-27N and Wall-34N) the vertical reinforcement had a lapse length of 800mm with 10mm diameter dowels protruding from the R/C foundation block. The cells hosting the vertical reinforcement were the only ones grouted being previously properly cleaned. In all cases the horizontal reinforcement was embedded within the mortar of the bed-joints. For most specimens reinforcing rods of 4.0mm diameter were used as shown in Figure 4 for Wall-27N. Alternatively, the

maximum diameter of the transverse reinforcement was either 4.9mm or 5.5mm in some cases. The variation of the diameter of the horizontal reinforcing bars together with their placement either in every bed joint (Figure 4) or every other bed joint resulted in the variation of the transverse reinforcing ratio in the range from 0.05%, to 0.150%. In all cases of wall specimens with a nominal thickness of 154mm this transverse reinforcement was formed of two parallel reinforcing rods lying within the mortar at a distance of approximately 20mm from either façade of the wall specimen. During the loading sequence a number of sensors were employed together with a data acquisition system in order to record continuously the level of the applied horizontal and vertical forces as well as the horizontal, vertical and diagonal displacements at various points of the loaded specimens. Figure 4 depicts the used instrumentation scheme for specimen Wall-27N. During the loading sequence the level of the applied horizontal and vertical forces was monitored in real-time in-order to check at all-times the progress of the loading sequence and prohibit any possibility of accidental over-loading. Moreover, during all the stages of the test the development of damage was recorded at both sides of each wall specimen. Figure 6 showing the damage of Wall-27N represents the state of this specimen at the end of the loading sequence. The main types of damage that were recorded are the following: a) Breaking of a brick unit and disintegration of its outer face. b) Breaking and disintegration of the whole brick unit. c) Compression failure of the brick unit and grout fill at the toe of the wall. d) Rupture or buckling of the longitudinal reinforcements. The measured response during the cyclic tests of the partially grouted rein-forced walls has been treated in such a way as to deduce the most significant modes of deformation.

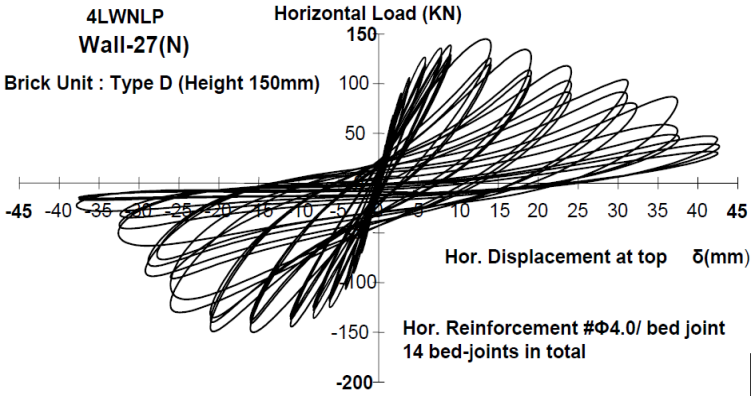

Figure 5: Overall cyclic response of specimen Wall-27N

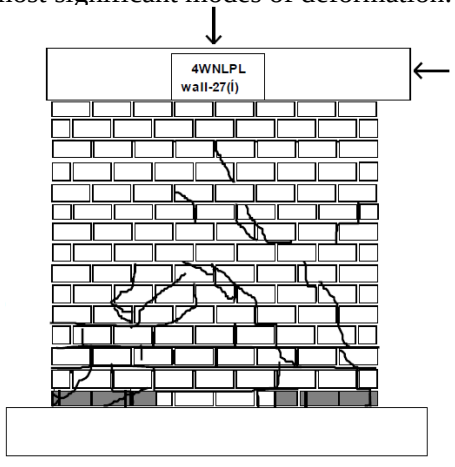

Figure 6: Wall-27N damage at end of all cycles

6. Observed response

The observed response of specimen Wall-27N (Figure 4) is presented, discussing the most significant features of the observed response for “wide” wall specimens with shear reinforcement ratio just below 0.1%. The influence of the varied parameters is included in the full report. Figure 5 portrays the overall measured response in terms of imposed horizontal load at the top of the specimen versus the corresponding horizontal displacement at the same location. As can be seen in this figure an initial approximately elastic behavior is evident with a stiffness value 27kN/mm in the range up to 4mm horizontal displacement and 110kN horizontal load. Next, the non-linear response of the specimen becomes evident till the maximum load value equal to 148kN is reached for an imposed horizontal displacement equal to 13mm. From this point any further increase in the imposed horizontal displacement (up to 40mm) is accompanied with a gradual deterioration of the horizontal load which reaches 25% of the maximum load at the end of test. Throughout all this cyclic loading sequence the response remains almost symmetric absorbing at the same time considerable plastic deformation energy, which is beneficial for the seismic resistance. The observed damage for Wall-27N (Figure 6) follows similar trends to the damage which was observed for “wide” wall specimens with height over length ratio approximately equal to 1. This is initially of flexural type, but as the imposed level of horizontal displacement increases the shear type of damage also becomes evident. However, for Wall-27N there was no disintegration of any part of the brick masonry within the wall. Moreover, the large

plastic rotation at the wall-foundation interface was accompanied with compression brick failures at the toes of the wall and with signs of overstress of the longitudinal reinforcement at these locations during the cycles after the maximum horizontal load was reached. The deterioration of the bearing capacity of Wall-27N must be attributed to the contribution of the shear response together with the disintegration of the compressive zones at the two toes of this wall during large plastic rotations (Figure 6). As with Wall-27N response, most of the specimens tested developed local compressive-type modes of failure. The main types of damage that were record-ed are breaking of a brick unit and disintegration of its outer face or of the whole brick unit and com-pression failure of the brick unit and grout fill at the toe of the wall. These modes of failure influence the overall seismic response and they are critical factor of the observed performance. Therefore, an additional objective was to produce an alternative clay brick unit in order to avoid such local compressive-type modes of failure. The various steps employed to achieve this objective are presented and discussed below (section 9).

7. Numerical simulation

An attempt is made here to numerically simulate the observed behavior of Wall-27N presented before. This was done employing a micro-modeling technique whereby the bricks were simulated by elastic plane finite elements separately from the simulation of the mortar bed and head joints and of the longitudinal reinforcement. A brief outline of this numerical simulation is presented together with a selection of the obtained results. The mortar joints in this micro-model are represented with non-linear link elements aimed to simulate the cut-off tensile capacity normal to the mortar joint-brick as well as the non-linear compressive behavior when, as was observed (Figure 6) the axial compression attains relatively large values at the narrow compressive zone along the toes of this wall. At this stage the numerical simulation does not simulate the non-linear shear response of the mortar-joint brick interface and the horizontal reinforcement nor the dowel action of the longitudinal reinforcement. Therefore, this type of the response that developed in Wall-27N, as shown by the relevant measurements, is not numerically simulated at present. The vertical reinforcement was simulated explicitly by including in the numerical model non-linear links with properties based on the measured mechanical tensile characteristics of the actual longitudinal reinforcement as these properties were measured (see section on material characterization). These non-linear links are at the same locations where the vertical reinforcing bars were placed and grouted within Wall-27N specimen (Figures 4 and 7).

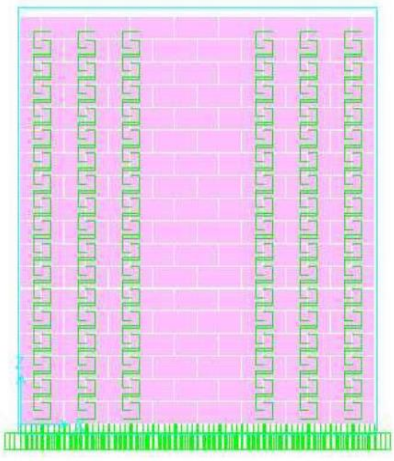

Figure 7: Links for reinforcing bars

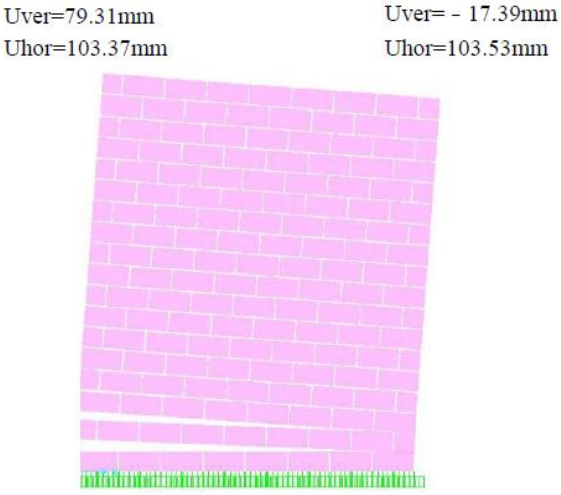

Figure 8: Wall deformation for vertical and horizontal loading. Deformations measured at the two ends of top section

Similarly, from the measured mortar mechanical characteristics the properties of the non-linear links representing the mortar joints were derived. The loading conditions of the experimental sequence were simplified in the numerical simulation through a step-by-step time history algorithm. Initially, the vertical load was applied gradually followed by the gradual application of the horizontal. At this stage the cyclic

nature of the horizontal loading sequence (Figure 3) was not simulated. Instead, in the present numerical simulation the horizontal load was applied in a monotonic fashion whereby this horizontal load was gradually increased from zero to a value approximating the maximum value attained during the experimental sequence. An alternative process would be to apply a gradually increasing horizontal top displacement.

Figure 9 depicts the deformation patterns as resulted from the described numerical simulation the vertical and horizontal loading. As can be seen in Figure 9 the observed during testing dominant plastic rotation at the region near the wall-foundation interface was successfully reproduced by this non-linear micro-modeling. In Figure 9 the overall response of Wall-27N specimen is depicted in terms of overturning moment at a horizontal section near the wall-foundation interface versus the horizontal displacement at the top of the specimen.

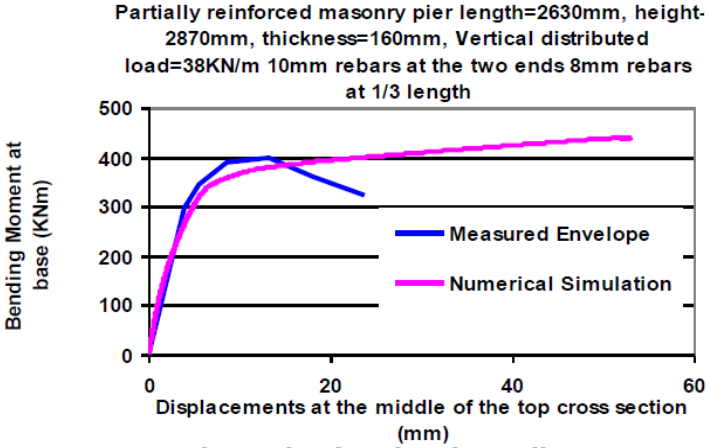

Figure 9: Observed and predicted overall response

The measured response is depicted as an envelope curve of the cyclic response depicted in Figure 6. As can be seen in Figure 10 the used numerical simulation predicted reasonably well the observed overall response up to the point of maximum overturning moment. From this point onwards the numerical simulation fails to re-produce the observed deterioration in the overall response. This is attributed to the fact that this numerical simulation does not represent any deterioration arising from the disintegration of the compressive zone, which was discussed in the previous section (Figure 6). Moreover, as already underlined, the used numerical simulation does not include at this stage any non-linearities arising from the shear response of the mortar joints. Figure 10 depicts the distribution of the normal stresses in the vertical direction (σ22) for Wall-27N specimen at the loading stage where the horizontal forces attain the maximum value (together with the vertical forces described before). As can be seen, this distribution of normal stresses in the vertical direction (σ22) is quite realistic showing, as expected, a narrow compressive zone at the right bottom toe of this masonry wall whereas the tensile forces at the mortar bed-joints at the left side of the wall attain very small values; instead, the reinforcing bars at this part develop, as expected, the required tensile forces (Figure 11).

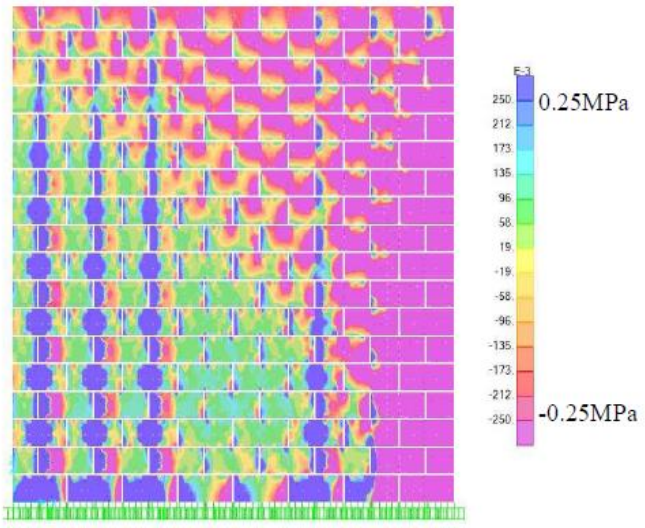

Figure 10: Normal stress distribution of masonry Wall-27N in the vertical direction

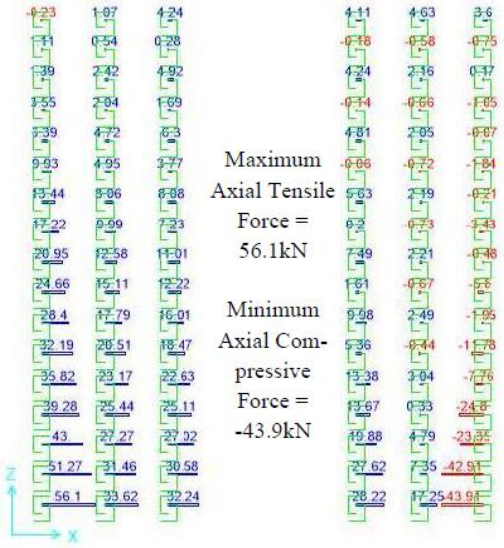

Figure 11: Distribution of axial forces of the links representing the longitudinal reinforcing bars.

8. Investigation of the behavior of the alternative clay brick unit

The methodology used to investigate the behavior of the new clay brick unit with vertical holes to be used for reinforced masonry low-rise buildings will be briefly presented here. First of all, an extensive experimental sequence was carried out focusing on monitoring basic properties of the ceramic material, that will be used to produce the new clay brick unit in the Laboratory of Strength of Materials and Structures, at Aristotle University. Specimens were subjected to either axial compression (figure 12) or four-point-bending tests (figure 14) in the laboratory, re-cording the brittle nature of their behavior together with the corresponding axial compression or flexural tensile strength. A 3-D non-linear finite element simulation of these tests was formed including all the geometrical, loading and support details, in an effort to numerically simulate the observed behavior. The numerical models captured successfully the measured brittle load-deformation response (figures 13, 15). Moreover, the observed actual damage at the end of the tests resembles the distribution of the plastic strains after the ultimate load is reached, as predicted by these numerical simulations.

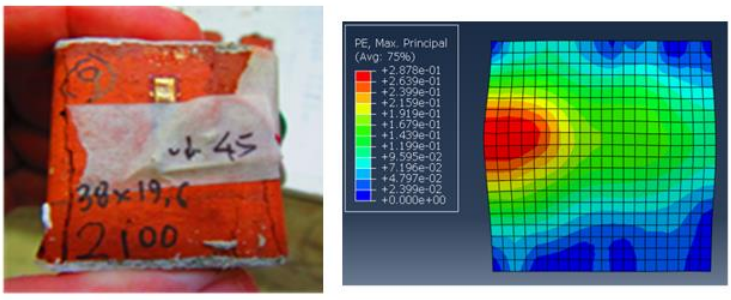

Figure 12: observed and numerically predicted damage patterns of the axial compression test,

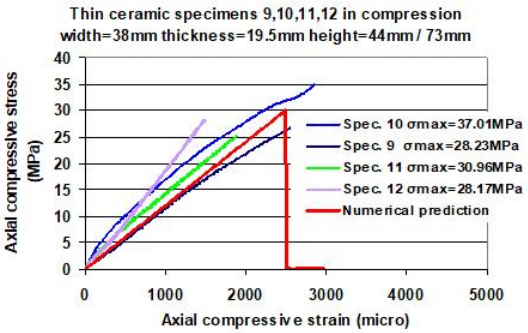

Figure 13: Stress-strain response measured during the axial compression tests

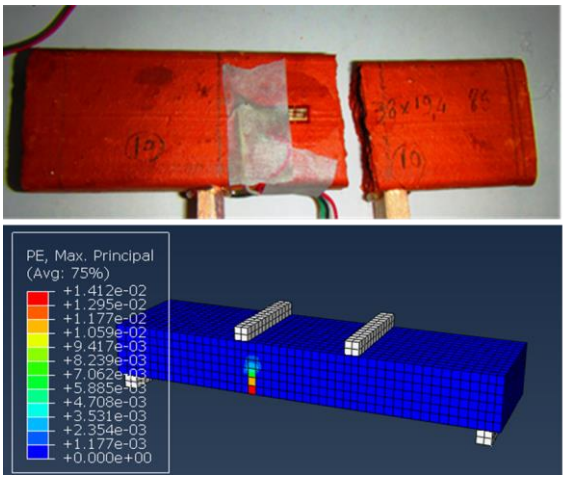

Figure 14: observed and numerically predicted damage patterns of the four-point bending test

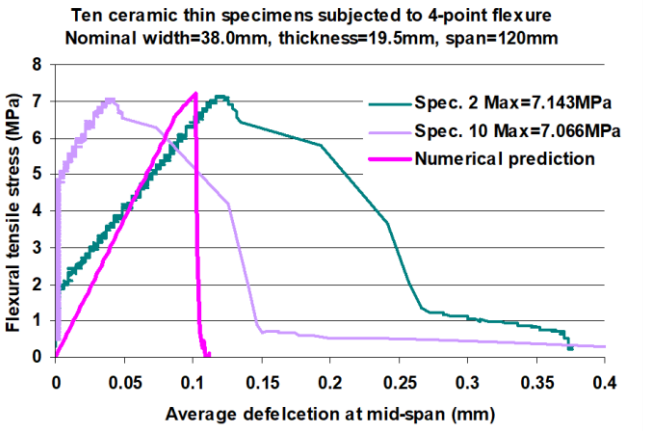

Figure 15: Stress-strain response measured during the four-point bending tests

Next, a number of clay bricks with vertical holes commercially produced was subjected to axial compression test. The geometrical details of the brick tested are shown in the figure below, figure 16. These specimens were subjected to compression according to the relative standard EN 772-1. The specimens were subjected to two different directions of compressive load. The first direction of loading is vertical to the direction of the bed joints (direction a-a). The second one is parallel to the direction of the bed joints (direction b-b).

A three dimensional (3-D) finite element representation of the axial compression test of the clay brick tested at the laboratory was formed. The same methodology is used, as it was used in the previously mentioned numerical simulations of the ceramic specimens. The presented results depicted in figure 16 are plots of the distribution of plastic strains with-in the volume of the numerical simulation when the ultimate load is reached. Additionally, a comparison between the observed behavior and the numerical predictions are shown below in figure 17, in terms of the maximum load reached for both loading conditions. In both cases there is a good agreement between the experimental results and the numerical predictions at maximum load reached. Therefore, this method can also be used with a degree of conformity for the design of a new clay brick unit with the desired geometry and the desired compressive strength to be used to partially grouted reinforced masonry buildings.

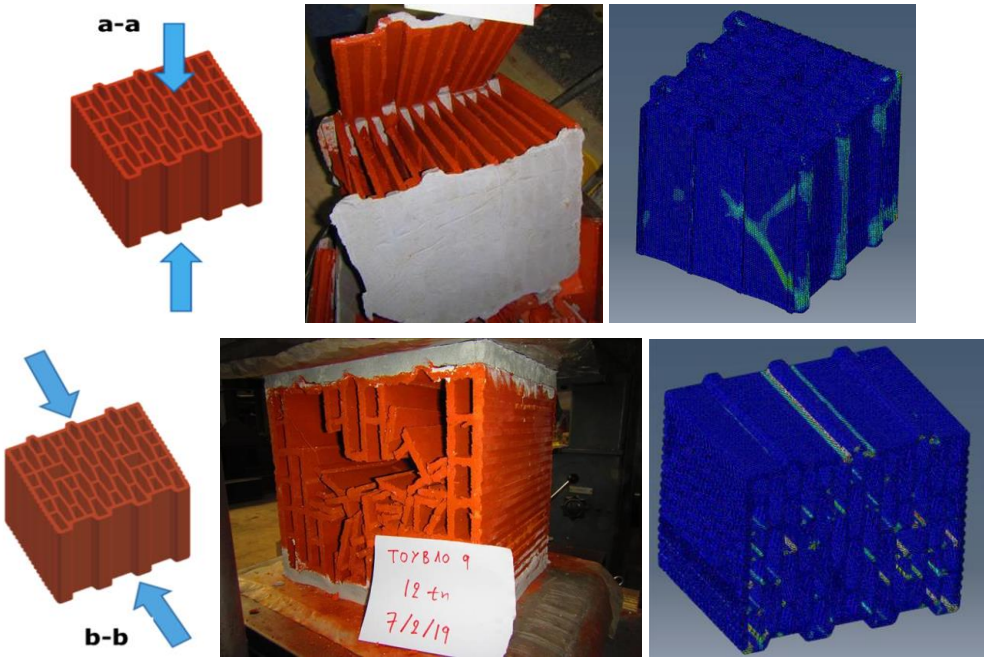

Figure 16: observed and numerically predicted damage patterns for the two different compression tests.

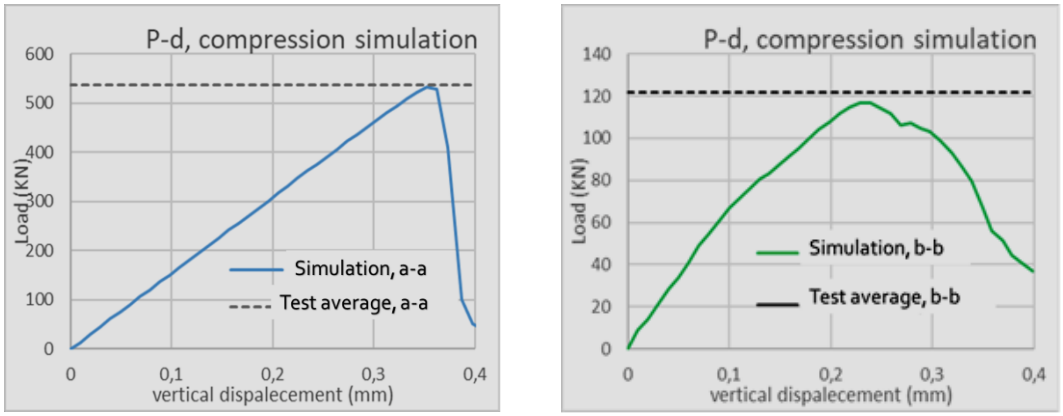

Figure 17: Comparison between experimentally measured response and numerical prediction for the two different compression tests.

Based on the numerical models developed before, an investigation about the specific geometrical properties (dimensions, shell thickness, arrangement of holes) of the new brick unit took place. The final geometry of the new brick is depicted in the picture below, figure 18. The numerical predictions of its compressive behavior parallel to the bed joint's direction is given in the diagram below, figure 18. The mean compressive strength of the new unit was predicted to 7.36 MPa according to EN 772-1. Afterwards this unit was

produced and a number of specimens were tested at the laboratory. More specific six specimens were subjected to axial compressive load perpendicular to the bed joint's direction. Three of these specimens were with bare holes while the other three had their holes filled with therm insulating material (EPS). The mean compressive stress calculated for these two types of the new unit is 7.90 MPa and 6.34 MPa respectively, table 2. The modes of failure of two specimens, one bare and one with filled holes are depicted in figure 19. Compared to the numerical predictions, the numerical model developed before predicted quite satisfactorily the behavior of the clay brick unit in terms of maximum stress developed and the mode of failure. Thus, this new unit has the desired mechanical and geometrical properties to be used for the construction of load bearing masonry buildings according to EN 1996-1-1.

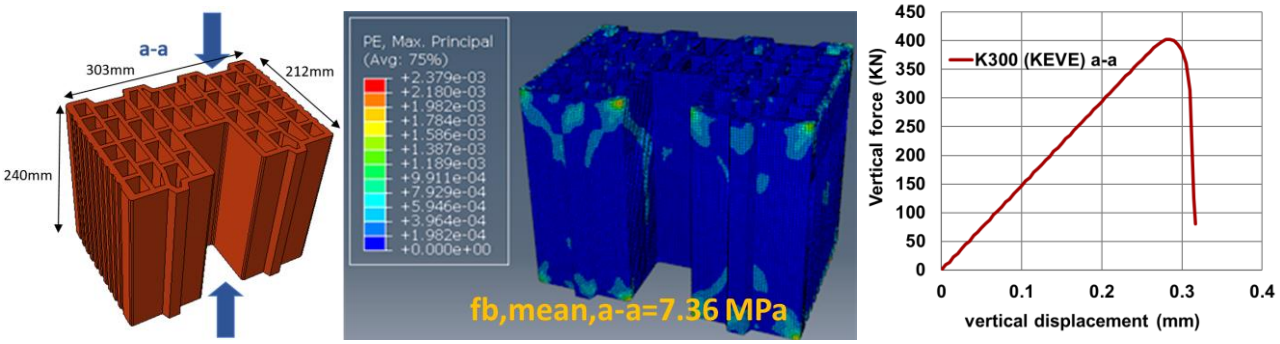

Figure 11: Geometry of the new brick unit (left) and the numerical predictions. The mode of failure (left) and the load – displacement response (right)

Figure 12: Modes of failure observed after compression test for the bare brick (left) and the filled with EPS brick (right)

Table 2: mean compressive strength derived by new brick's tests

Brick unit	average $\mathbf{f_b}$ mean (MPa)	standard deviation (MPa)
bare	7.90	0.87
Filled (EPS)	6.34	1.59

11. Conclusions

- A number of partially grouted reinforced brick masonry wall specimens, constructed with a brick unit produced by a Greek manufacturer, were subjected to vertical forces combined with horizontal cyclic seismic-type loads applied simultaneously. The longitudinal reinforcing ratio was 0.12% whereas the horizontal reinforcing ratio was varied in the range from 0.05%, to 0.15%. For the tested walls, with a height over length ratio equal to 1 and for horizontal rein-forcing ratio values larger than 0.085%, the flexural response together with the rather ductile plastic rotation response at the bottom of the wall, similar to a plastic-hinge mechanism, appeared to dominate the observed behavior when the maximum horizontal load was reached.

- This observed mainly flexural behavior was successfully reproduced by a micro-modeling numerical simulation featuring all the geometric and construction detailing together with the measured non-linear mechanical characteristics of the mortar joints and the vertical reinforcing bars of the described Wall-27N specimen.

- A critical factor of the observed performance was the behavior of the employed clay brick unit which developed local compressive-type modes of failure, which influence the overall seismic response. Therefore, an additional objective was to develop a similar clay brick with enhanced compressive behaviour. The methodology used to investigate the behavior of the new clay brick unit is briefly presented here.

10. Acknowledgements

All materials for the construction of the specimens were provided by "KEBE S.A. (Northern Greece Ceramics)". Part of the aforementioned research has been co-funded by Greece and European Union through the Operational Program "Erevno - Dimiourgo - Kainotomo" which are gratefully acknowledged.

European Union
European Regional Development Fund
HELLENIC REPUBLIC
MINISTRY OF ECONOMY & DEVELOPMENT
SPECIAL SECRETARY FOR ERDF & CF
MANAGING AUTHORITY OF EPAnEK
EPAnEK 2014-2020
OPERATIONAL PROGRAMME
COMPETITIVENESS
ENTREPRENEURSHIP
INNOVATION
ΕΣΠΑ 2014-2020
ανάπτυξη - εργασία - αλληλεγγύη
Partnership Agreement 2014 - 2020
Co-financed by Greece and the European Union

12. References

[1] Computers and Structures Inc. (2010), Structural and Earthquake Engineering Software.

[2] Eurocode 6, (2005), "Design of masonry structures - Part 1-1: General rules for reinforced and unrein-forced masonry structures".

[3] EUROPEAN STANDARD EN 772-1, (2011), "Methods of test for masonry units - Part 1: Determination of compressive strength, May 2011

[4] Gulkan P., et al. (1990) "Seismic Testing of Single-story Masonry Houses: Parts 1 and 2", Journal of Structural Engineering ASCE, Vol. 116, No 1, January 1990, pp. 235-274.

[5] Hidalgo, P. A., et al. (1978), "Cyclic Loading Tests of Masonry Single Piers", EERC Reports No. 78/27, 78/28, 79/12, University of California at Berkeley.

[6] Manos, G.C., (1983), "Shaking Table Study of Single-Story Masonry Houses", EERC Report No. 83/11, University of California, Berkeley, U.S.A.

[7] Manos, G.C., (2000a) "The earthquake performance of partially reinforced masonry piers subjected to in plane cyclic loading", Report to the Greek General Secretariat of Research and Technology (in Greek).

[8] Manos, G.C., et al. (2000b), "The observed performance of partially reinforced masonry piers subjected to combined horizontal cyclic and compressive loads." 12th World Conference Earthquake Engineering.

[9] Manos, G.C., et al. (2001) "The earthquake performance of partially reinforced masonry piers subjected to in-plane cyclic loading", 9th Canadian Conference of Masonry Structures.

[10] Modena, C., et al. (1996), "Reinforced Masonry for Buildings in Seismic Zone", Report of University of Padova in the framework of Brite Euram Project No 4001.

[11] Oan, A.F, Shrive, N.G. (2009), "Shear of concrete masonry walls". 11th Canadian Masonry Symposium, Toronto, Ontario.

[12] Psilla, N., (1996), "Seismic Behavior of Rein-forced Masonry", Greek Conference on Reinforced Concrete Structures, Vol. II, pp. 284-294, Cyprus, (in Greek).

[13] Sandoval, C., Calderón, S., Almazán, J.L. (2018). "Experimental cyclic response assessment of partially grouted reinforced clay brick masonry walls". Bulletin of Earthquake Engineering, 16(7): 3127-3152.

[14] Tasios, T. P., (1987), "The Mechanics of Masonry", Athens, (in Greek)

[15] Tomazevic, M., et al. (1993), "In-Plane Behavior of Reinforced Masonry Walls Subjected to Cyclic Lateral Loads", Reports ZRMK/PI-92/06 and 08, Institute ZRMK, Ljubljana, Slovenia.

